Available online at www.sciencedirect.com
ScienceDirect
Polymer 47 (2006) 6868–6873
polymer
www.elsevier.com/locate/polymer

Pure shear deformation of physical and chemical gels of poly(vinyl alcohol)

Kenji Urayama*, Satoru Ogasawara, Toshikazu Takigawa

Department of Materials Chemistry, Kyoto University, Kyoto 615-8510, Japan

Received 9 June 2006; received in revised form 12 July 2006; accepted 13 July 2006
Available online 2 August 2006

Abstract

Pure shear deformation reveals the significant differences in elastic properties of the poly(vinyl alcohol) (PVA) gels with almost identical initial modulus, but with different types of crosslinks, physical crosslinks formed by microcrystallites and chemical crosslinks made of covalent bonds. The ratio of the two principal stresses steeply increases with elongation in the physical gels, while that remains almost constant independently of stretching in the chemical gels. The marked growth of the stress ratio with elongation in the physical gels leads to the negative values of the derivative of the elastic free energy (W_2) with respect to the second invariant of the deformation tensor in the whole range of deformation, which is firstly observed for elastomeric materials. By contrast, the chemical gels exhibit the positive values of W_2 like most chemically crosslinked rubbers. Among the existing theories of rubber elasticity, the classical non-Gaussian three-chain model considering the effect of finite chain-length is qualitatively successful in accounting for the steep increase of the stress ratio and the negative values of W_2 in the physical gels, although it fails to reproduce the large difference in the stress–strain behavior among uniaxial, pure shear and equibiaxial deformations. These features of the physical gels are expected to stem from the structural characteristics such as fewer amounts of slippery-trapped entanglement along network strands compared to the chemical PVA gels.

Keywords: Gel; Poly(vinyl alcohol); Rubber elasticity

1. Introduction

Polymer gels are conventionally categorized into two groups according to the types of crosslinking, i.e., chemical gels and physical gels [1,2]. Crosslinks in chemical gels are made of covalent bonds, while those in physical gels are formed by non-covalent bonds such as microcrystallites, glassy domains and helical structures. Poly(vinyl alcohol) (PVA) is capable of forming the chemical or physical gels depending on the preparation schemes. Hyon et al. [3] reported that the transparent physical PVA gels with high tensile strength and elongation at break are obtained by cooling the PVA solutions at sufficiently low temperatures using a mixture of dimethylsulfoxide (DMSO) and water (4:1 by weight) as the solvent. Crosslinks of the resulting gels are made of microcrystallites of PVA. We reported uniaxial tensile properties of the physical PVA gels in the previous papers [4,5]. Network structures of the physical PVA gels strongly depend on solvents and gelation temperature. It was reported [6,7] that in the case of the mixture solvents of DMSO and water with other mixing ratios and/or higher gelation temperatures, the opaque gels with heterogeneous structure are formed as a result of a competition between phase separation and gelation. We treat here the physical PVA gels prepared by the method of Hyon et al. Their method yields the gels with transparent appearance and homogeneous structure since the rate of network formation is so fast that the phase separation can be effectively suppressed [6,7]. This gel does not show the upturn of scattering intensity at low scattering vectors indicating a heterogeneous structure, unlike the physical PVA gels prepared using other solvent compositions [6] and most of gel systems [8].

The chemical and physical gels are expected to differ significantly in mechanical properties as well as network structure; however, there exists no report comparing the mechanical

* Corresponding author. Tel.: +81 75 383 2454; fax: +81 75 383 2458.
E-mail address: urayama@rheogate.polym.kyoto-u.ac.jp (K. Urayama).

0032-3861/$ - see front matter © 2006 Elsevier Ltd. All rights reserved.
doi:10.1016/j.polymer.2006.07.021

behavior of the physical and chemical gels having the same chemical structure regarding polymer network backbones. In the present study, we investigate the tensile behavior of the physical and chemical PVA gels under the three different modes of deformation: uniaxial, equi-biaxial and pure shear deformations. Uniaxial deformation has often been employed in the earlier studies because of the experimental simplicity. Uniaxial deformation, however, provides limited information because it is only a particular case among physically possible deformations of gels. Other deformation modes such as biaxial deformation are needed for full characterization of mechanical properties. Several studies showed the importance of biaxial stretching in the characterization of the elastic free energy governing the stress–strain behavior [9–15]. Most of these studies have focused on chemically crosslinked rubbers, and there is no study on biaxial stress–strain behavior of physical gels to our knowledge. Among biaxial deformations, pure shear (constrained uniaxial) deformation is of significance, because it corresponds to an intermediate between uniaxial and equi-biaxial stretching: in pure shear deformation, a sample is uniaxially elongated while the dimension along one principal axis is kept constant during stretching. In the present paper, we demonstrate that pure shear deformation clearly reveals the marked differences in tensile behavior of the physical and chemical PVA gels.

2. Experimental section

2.1. Poly(vinyl alcohol) (PVA)

PVA was kindly supplied by Unitika Co. (Japan). The number of repeating monomer units and the degree of saponification are 1700 and 99.5 mol%, respectively.

2.2. Preparation of physical PVA gels (P-GEL)

PVA was dissolved in a mixture of DMSO and water with the mixing ratio of 4:1 by weight. The solution was poured into a metal mold, and kept at −20 °C for 24 h for gelation. This gelation time was sufficiently long to achieve the quasi-equilibrium, because the gelation time over 24 h did not appreciably influence the elastic modulus of the resulting gels. The PVA concentrations were 12 and 15 wt%, and the resultant gels are designated as P-GEL-12 and P-GEL-15, respectively.

2.3. Preparation of chemical PVA gels (C-GEL)

Glutaraldehyde (GA) was mixed with the aqueous PVA solution so that the molar ratio of repeating units of PVA to GA could be 250/1. The reaction was carried out after the method of Horkay and Zrínyi [16]. The solutions with pH = 1.5 were poured into the metal mold, and maintained overnight at 25 °C for crosslinking reaction. The three gels designated as C-GEL-7.5, C-GEL-10 and C-GEL-12 were prepared from the solutions with 7.5, 10 and 12 wt% of PVA, respectively.

2.4. Tensile measurements

The P-GEL and C-GEL samples removed from the molds were used for the tensile measurements. All tensile measurements for each gel were completed within 5 h just after removing the gel from the mold to obtain the data with good reproducibility excluding the effect of aging (syneresis) whose time scale is in the order of day. Pure shear and equi-biaxial deformations of the sheet samples with 50 mm × 50 mm × 1.2 mm were carried out with BISS-0404 (Iwamoto Seisakusyo, Japan) at 25 °C. The samples are stretched in the two orthogonal directions (x and y directions). The principal ratio λ_i ($i = x,y,z$) is defined as $\lambda_i = l_i/l_{i0}$ where l_i and l_{i0} are the lengths along the i axis in the deformed and undeformed states, respectively. In equi-biaxial stretching, the samples were equally elongated in the x and y directions (i.e., $\lambda_x = \lambda_y$). In pure shear deformation, the samples were stretched in the x direction with maintaining the initial dimension in the y direction (i.e., $\lambda_y = 1$). The crosshead speed (v) was 1.0 mm/s.

Uniaxial elongation of the samples with 10 mm (width) × 50 mm (length) × 1.2 mm (thickness) was conducted with Tensilon RTM-250 (Orientec, Japan). The crosshead speed was 0.83 mm/s. The initial strain rate defined by v/l_{x0} (≈ 0.02) is almost identical in uniaxial and biaxial deformations. The previous study confirmed that the tensile behavior of P-GEL was almost independent of the initial strain rate in the wide range of $4 \times 10^{-4} < v/l_{x0} < 0.2$ [5].

3. Results and discussion

Figs. 1 and 2 display principal stresses σ_i ($i = x,y$) as a function of λ_x for P-GEL-15 and C-GEL-10 under uniaxial, pure shear and equi-biaxial deformations, respectively. The stress in the figures is the nominal stress defined by the force per unit cross-sectional area in the undeformed state. For both gels, the stresses at the same λ_x considerably differ between

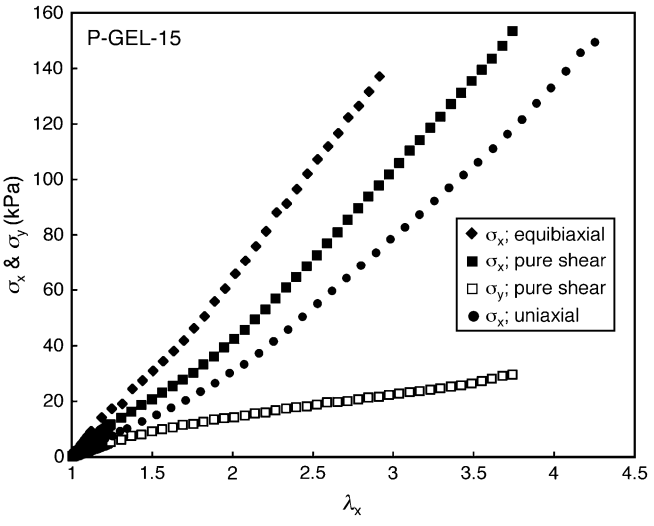

Fig. 1. Principal stresses (σ_x and σ_y) as a function of λ_x in equi-biaxial, pure shear and uniaxial deformations for P-GEL-15.

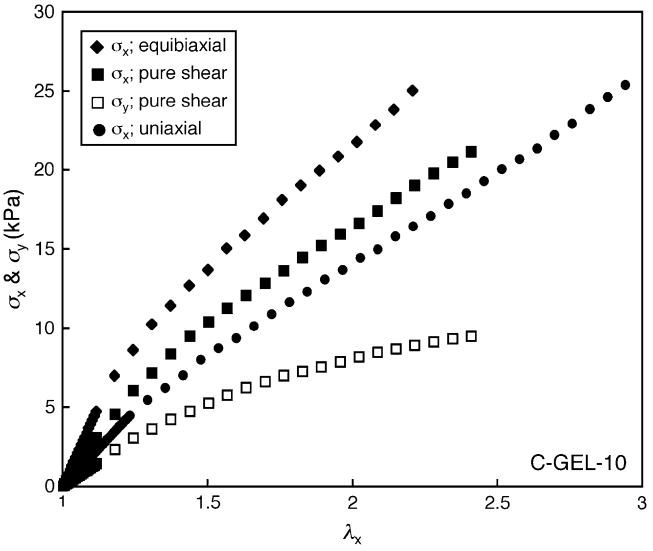

Fig. 2. Principal stresses (σ_x and σ_y) as a function of λ_x in equi-biaxial, pure shear and uniaxial deformations for C-GEL-10.

the three types of deformation in the whole range of λ_x: in order of magnitude, σ_x (equi-biaxial) $> \sigma_x$ (pure shear) $> \sigma_x$ (uniaxial) $> \sigma_y$ (pure shear). In equi-biaxial stretching, σ_y is identical with σ_x within the experimental error for both gels. At small elongation of $\lambda_x < 1.1$, σ_i ($i = x,y$) is proportional to strain as $\sigma_i = A\ (\lambda_x - 1)$ in each deformation. The coefficient A in each deformation is listed in Table 1. The linear elasticity theory [17] for incompressible materials yields the following relations: $A_x = A_y = 6G$ for equi-biaxial deformation; $A_x = 4G$ and $A_y = 2G$ for pure deformation; and $A_x = E = 3G$ for uniaxial deformation where G and E are shear modulus and Young's modulus, respectively. The relation between the moduli in the experiments is fairly close to but appreciably different from the theoretical expectation. A deviation from the theoretical ratio is attributed to the experimental error and a finite compressibility which will be described later. Importantly, the moduli of the P-GEL and C-GEL samples are comparable, and in particular, P-GEL-15 has almost the same modulus as C-GEL-12. This indicates that the two systems are similar in the density of elastically effective network strands including the contributions of chemical crosslinks and trapped entanglements, which enables us to focus the influence purely stemming from crosslinking types on stress–strain behavior.

The shape of the $\sigma-\lambda$ curves for P-GEL-15 is different from that for C-GEL-10. The curves for P-GEL-15 are slightly convex, while those for C-GEL-10 are somewhat concave. These characteristics depend on whether the gel is crosslinked chemically or physically, although the data for other samples are not shown here. A remarkable difference in tensile behavior of the physical and chemical gels appears in the stress ratio (σ_x/σ_y) under pure shear deformation, which is shown in Fig. 3. The stress ratio for all C-GEL samples lies around two in the whole λ_x region, while that steeply increases with λ_x for the P-GEL samples. The growth of σ_x/σ_y in the physical gels is mainly due to a steep increase of σ_x with elongation since the λ_x dependence of σ_y is weak. An inflection of the curve at $\lambda_x \approx 2.5$ for P-GEL-15 or at $\lambda_x \approx 3$ for P-GEL-12 results from an irreversible structural change caused by large elongation. Perfect recovery of the original length after releasing the applied strain was not achieved for P-GEL-15 and P-GEL-12 when stretched over the inflection points. Large stretching over $\lambda_x \approx 2.5$ will cause a rupture of microcrystalline domains acting as crosslinks. The occurrence of the strain-induced crystallization cannot be ruled out; however, it should be noted that this possibility holds for both P-GEL and C-GEL because they are almost similar in crosslinking density. In addition, a significant difference in σ_x/σ_y for P-GEL and C-GEL is observed even at small elongation of $\lambda_x \approx 1.5$, not limited in high stretching region. The strain-induced crystallization is not

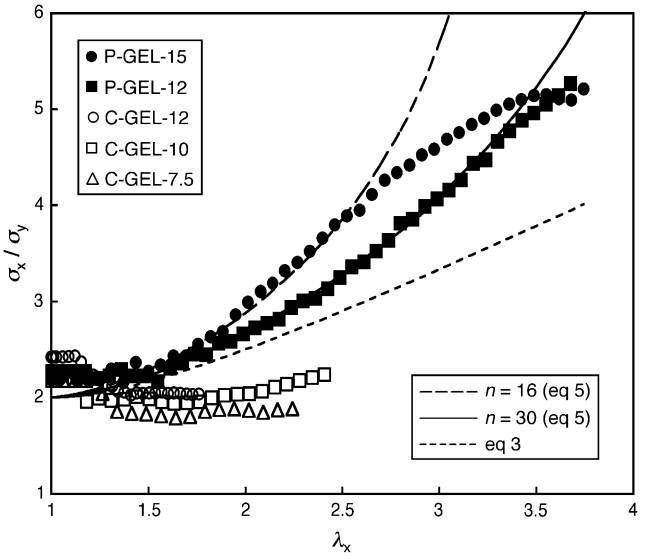

Fig. 3. Stress ratio (σ_x/σ_y) as a function of λ_x in pure shear deformation for each sample. The dashed and solid lines represent the results of three-chain non-Gaussian network theories with $n = 16$ and 30, respectively. The dotted line corresponds to the prediction of classical theories of rubber elasticity and the condition of $W_2 = 0$.

Table 1
Linear elastic constants in various deformations for each sample

	Equi-biaxial		Uniaxial	Pure shear		
	A_x (Pa)	A_y (Pa)	A_x (Pa)	A_x (Pa)	A_y (Pa)	A_y/A_x
P-GEL-12				1.64×10^4	7.22×10^3	0.440
P-GEL-15	7.60×10^4	7.60×10^4	3.44×10^4	4.74×10^4	2.18×10^4	0.460
C-GEL-7.5				8.53×10^3	3.92×10^3	0.460
C-GEL-10	4.08×10^4	4.01×10^4	1.92×10^4	2.64×10^4	1.22×10^4	0.460
C-GEL-12				4.21×10^4	1.74×10^4	0.413

a primary origin for the significant difference in the tensile behavior of P-GEL and C-GEL.

According to the linear elasticity theory, [17] the stress ratio σ_x/σ_y in the small strain limit under pure shear deformation corresponds to the inverse of Poisson's ratio (μ): $\sigma_y/\sigma_x = \mu$. The values of μ estimated from the limiting value of σ_y/σ_x are listed in Table 1. The values of μ for all samples are slightly smaller than 1/2, indicating a finite compressibility. The values of μ for the P-GEL samples are comparable to those evaluated from the dimensional variations in uniaxial stretching in our previous study [5].

Let us compare the λ_x dependence of σ_x/σ_y in the experiments with the prediction of the classical theory of rubber elasticity. The elastic free energy density (W) in the classical theory on the basis of the Gaussian-chain approximation is expressed as [18]

$$W = \frac{\nu kT}{2}\left(\lambda_x^2 + \lambda_y^2 + \lambda_z^2 - 3\right) \tag{1}$$

where k is Boltzmann's constant, T is the absolute temperature, and ν is the number density of elastic chains in the affine model or the cycle rank in the phantom model [18]. The quantity ν is correlated with the molecular mass between adjacent elastically effective junctions (M_x) and the concentration of elastically effective network strands (c_N) as $\nu = c_N N_A kT/M_x$ where N_A is Avogadro's number. Eq. (1) yields the expressions for σ_x and σ_y in pure shear deformation as

$$\sigma_x = \nu kT\left(\lambda_x - \frac{1}{\lambda_x^3}\right) \tag{2a}$$

$$\sigma_y = \nu kT\left(1 - \frac{1}{\lambda_x^2}\right) \tag{2b}$$

The stress ratio σ_x/σ_y is given by

$$\frac{\sigma_x}{\sigma_y} = \lambda_x + \frac{1}{\lambda_x} \tag{3}$$

The dotted line in Fig. 3 depicts σ_x/σ_y predicted by the classical theory (Eq. (3)). In sufficiently large λ_x region, the line is located between the data of the physical and chemical gels. The λ_x dependence of σ_x/σ_y by the classical theory is positive, but much weaker than that of the physical gels. By contrast, the chemical gels show almost no λ_x dependence of σ_x/σ_y in disagreement with the theoretical expectation. Non-Gaussian network theories [18–22] have been developed to model the effect of finite chain-length which is not considered in the classical theories, and they have often been used to account for the steep upturn of stress at high elongation observed for conventional elastomers. The three-chain model is the simplest version among the existing non-Gaussian theories. The expression of W for the three-chain model is [18]

$$W = \frac{\nu kTn}{3}\left[\sum_{i=x,y,z}\left\{\frac{\lambda_i}{n^{1/2}}L^{-1}\left(\frac{\lambda_i}{n^{1/2}}\right) + \ln\frac{L^{-1}\left(\lambda_i/n^{1/2}\right)}{\sinh L^{-1}\left(\lambda_i/n^{1/2}\right)}\right\} - 3\right] \tag{4}$$

where n is the number of segments for a single network strand and $L^{-1}(y)$ is the inverse Langevin function. The principal stresses under pure shear deformation in this model are given by

$$\sigma_x = \frac{\nu kTn^{1/2}}{3}\left[L^{-1}\left(\frac{\lambda_x}{n^{1/2}}\right) - \frac{1}{\lambda_x^2}L^{-1}\left(\frac{1}{\lambda_x n^{1/2}}\right)\right] \tag{5a}$$

$$\sigma_y = \frac{\nu kTn^{1/2}}{3}\left[L^{-1}\left(\frac{1}{n^{1/2}}\right) - \frac{1}{\lambda_x}L^{-1}\left(\frac{1}{\lambda_x n^{1/2}}\right)\right] \tag{5b}$$

Eqs. (5a) and (5b) yield a stronger λ_x dependence of σ_x/σ_y than Eq. (3) of the Gaussian-chain model at moderate and large stretching, while Eqs. (5a) and (5b) agree with Eqs. (2a) and (2b) at sufficiently small deformation. The results of the data-fitting by Eqs. (5a) and (5b) are represented by the dashed and solid lines in Fig. 3. The fitted curves well describe the steep increase of σ_x/σ_y for P-GEL-12 and P-GEL-15 in the region up to $\lambda_x \approx 3$ and $\lambda_x \approx 2.5$, respectively, beyond which an irreversible structural change by elongation occurs. The successful fit suggests that the sharp upturn of the stress ratio in the physical gels is primarily attributed to the finite chain-length effect. It is reasonable that the fitted value of $n = 30$ for P-GEL-12 is larger than $n = 16$ for P-GEL-15, since n^{-1} is proportional to initial modulus. In principle, n should be proportional to the number of the Kuhn segments for a single network strand (m). The affine model relates m to the initial modulus: $G = \nu kT = c_N N_A kT/(m_q M_0)$ where q is the number of real segments per Kuhn segment, M_0 is the molecular weight per repeating unit. When we employ the PVA concentration in the feed (c) as c_N, the resultant values are $m \approx 310$ for P-GEL-12 and $m \approx 140$ for P-GEL-15, both of which are fairly larger than the fitted values of n in Fig. 3. The Kuhn segment correlated with the chain dimension in the isolated and unperturbed state is not necessarily equivalent to the segment in the distorted non-Gaussian network chain [18]. In addition, the estimated values of m for the physical gels involve uncertainty because a considerable number of segments belong to microcrystalline domains acting as crosslinks, and we neglect here the presence of free chains and dangling chains that have no contribution to network elasticity. The real value of c_N in the physical gels becomes considerably smaller than c, if we consider these effects. That is why this calculation tends to overestimate the values of m. Nevertheless, it should be noted that P-GEL-12 and P-GEL-15 exhibit almost identical ratios of m/n (≈ 10). This indicates that the different samples have the same correlation between m and n, which supports the validity of the present approach.

The marked increase in σ_x/σ_y in the physical gels yields another interesting characteristic in elastic free energy. When W is expressed as a function of the first and second invariants of the deformation tensor (I_1 and I_2), biaxial stress–strain

relations are related to the derivatives of W with respect to I_1 and I_2 [18]:

$$W_1 \equiv \frac{\partial W}{\partial I_1} = \frac{1}{2\left(\lambda_x^2 - \lambda_y^2\right)}\left[\frac{\lambda_x^3\sigma_x}{\lambda_x^2 - \left(\lambda_x\lambda_y\right)^{-2}} - \frac{\lambda_y^3\sigma_y}{\lambda_y^2 - \left(\lambda_x\lambda_y\right)^{-2}}\right] \quad (6a)$$

$$W_2 \equiv \frac{\partial W}{\partial I_2} = \frac{-1}{2\left(\lambda_x^2 - \lambda_y^2\right)}\left[\frac{\lambda_x\sigma_x}{\lambda_x^2 - \left(\lambda_x\lambda_y\right)^{-2}} - \frac{\lambda_y\sigma_y}{\lambda_y^2 - \left(\lambda_x\lambda_y\right)^{-2}}\right] \quad (6b)$$

where $I_1 = \lambda_1^2 + \lambda_2^2 + \lambda_3^2$ and $I_2 = \lambda_1^2\lambda_2^2 + \lambda_2^2\lambda_3^2 + \lambda_3^2\lambda_1^2$. The third invariant $I_3 = \lambda_1^2\lambda_2^2\lambda_3^2$ is unity, since we assume here the incompressibility of the materials for simplicity. Although the form of $W(I_1,I_2)$ is usually unknown, biaxial stress–strain data provide us $\partial W/\partial I_i$ as a function of I_i $(i = 1,2)$ which is an important basis for deducing the form. It should be noticed that Eqs. (6a) and (6b) are undefined for uniaxial $\lambda_y = \lambda_x^{-1/2}$ and equi-biaxial $(\lambda_x = \lambda_y)$ stretching. The expressions of W_1 and W_2 for pure shear deformation $(\lambda_y = 1, I_1 = I_2)$ are given by

$$W_1 = \frac{1}{2\left(\lambda_x^2 - 1\right)}\left(\frac{\lambda_x^3\sigma_x}{\lambda_x^2 - \lambda_x^{-2}} - \frac{\sigma_y}{1 - \lambda_x^{-2}}\right) \quad (7a)$$

$$W_2 = \frac{-1}{2\left(\lambda_x^2 - 1\right)}\left(\frac{\lambda_x\sigma_x}{\lambda_x^2 - \lambda_x^{-2}} - \frac{\sigma_y}{1 - \lambda_x^{-2}}\right) \quad (7b)$$

The $I_1(=I_2)$ dependence of W_1 and W_2 for each sample is illustrated in Fig. 4. The data are reduced by the initial shear modulus of each sample. For both physical and chemical gels, W_1 and W_2 in the small strain limit exhibit upswing and downswing, respectively, which has often been observed for various elastomers [9–15]. A study [12] explains this as the asymptotic behavior toward a limiting value derived from the linear elasticity theory considering a finite compressibility. At the relatively large deformations of $I_1 > 4$, W_1 and W_2 for the chemical gels are positive, and they are almost independent or weakly dependent of I_1 like various chemically crosslinked elastomers [9–15]. By contrast, for the physical gels, W_1 grows with I_1. The curves of W_1 for P-GEL-12 and P-GEL-15 exhibit an inflection around $I_1 = 11$ and $I_1 = 9$, respectively. It should be recalled that the upper limit for perfectly recoverable deformation of P-GEL-12 and P-GEL-15 is $\lambda_x \approx 3$ and $\lambda_x \approx 2.5$ corresponding to $I_1 \approx 10$ and $I_1 \approx 8$, respectively. The inflection in the curve of W_1 is due to an irreversible change in network structure by elongation. Most interestingly, the values of W_2 for the physical gels are negative in the whole range of deformation. To our knowledge, this is the first observation of negative values of W_2 at large deformation, although W_2 for various elastomers becomes negative at the small deformation at $I_1 < 3.5$ [9–15].

The stress ratio in pure shear deformation satisfying $W_2 = 0$ is simply derived from Eq. (7b) as $\sigma_x/\sigma_y = \lambda_x + \lambda_x^{-1}$ which is identical with the relation from the classical theory (Eq. (3)). The solid line (Eq. (3)) in Fig. 3 also corresponds to the boundary of $W_2 = 0$. The derivative W_2 is positive or negative in the region below or beyond the boundary in the figure,

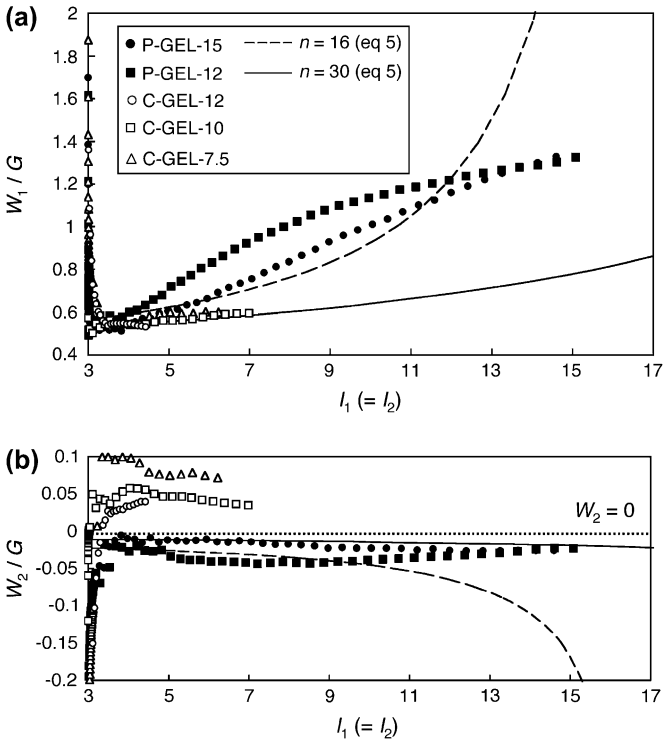

Fig. 4. The derivatives (a) W_1 and (b) W_2 as a function of I_1 $(=I_2)$ for each sample. The data are reduced by the initial modulus of each sample. The dashed and solid lines represent the results of three-chain non-Gaussian network theories with $n = 16$ and 30, respectively.

respectively. Most of the real elastomers including the chemical PVA gels exhibit finite and positive values of W_2 in discord with the prediction of the classical theory $(W_2 = 0)$ [9–15]. The origin of positive W_2 has often been explained in terms of trapped-entanglement effects of network strands which are not considered in the classical theory. Many entanglement models of rubber elasticity have been proposed, and most of them qualitatively accounts for positive W_2 at large deformation [23,24]. No entanglement model, however, yields negative W_2, which implies that entanglement effect is incapable of explaining negative W_2 in the physical PVA gels. As is evident in Fig. 3, negative W_2 results from large values of stress ratio. The lines in Fig. 4 denote the derivatives by the three-chain non-Gaussian model with the same fitted values in Fig. 3. Quantitative agreement of the theory and the data of the derivatives for the physical gels is not satisfactory, but the theory is qualitatively successful in explaining the negative values of W_2, suggesting that they mainly stem from the finite chain-length effect. There are several versions of non-Gaussian network models, [18–22] and the three-chain model is the simplest version among them. None of them consider explicitly the effect of trapped entanglements. Mao [22] derived a strict expression of W for a network of non-Gaussian chains which is applicable at moderate or low elongation. Mao showed that the model yields negative values of W_2 at small deformation, but the mathematical complexity prevents us from confirming that W_2 of the model is still negative at large deformation. Primitive-path model [20] and eight-chain model [21] are also an extension of the three-chain model,

and they consider a coupling of the deformations along different principal axes which is absent in the three-chain model. Both models, however, yield the same equation for σ_x/σ_y as Eq. (3) for pure shear deformation, i.e., $W_2 = 0$. It appears that among the existing theories, only the three-chain non-Gaussian model accounts for negative values of W_2 at large deformation. A striking shortcoming of the three-chain model is to yield no appreciable difference in σ_x at large elongation among uniaxial, pure shear and equi-biaxial deformations as a direct consequence of no coupling between the distortions along different principal axes. The three-chain model fails to describe the dependence of stress on the modes of deformation at high stretching. To describe the noticeable dependence of stress on the deformation modes as well as the negative values of W_2 in the physical PVA gels, we need a non-Gaussian network model considering a finite, but much weaker coupling of the deformations in different directions than the earlier approaches.

These significantly different stress–strain behaviors of the physical and chemical gels result from the differences in network structures. The larger stress ratio of P-GEL cannot be explained by the strain-induced crystallization. The P-GEL and C-GEL are similar in the amount of elastically effective junction, and they are stretched to the similar principal ratio ($\lambda \approx 2.5$). There is no reason why the strain-induced crystallization occurs only in P-GEL. It should be emphasized that the PVA concentrations before gelation (c) are sufficiently high to form the entanglement couplings of different precursor chains, because the values of c/c^* exceed 5 where $c^*(\approx 1.3$ wt%) [25] is the critical concentration for overlapping of the precursors employed. In general, the critical concentration for forming elastically effective entanglements is a few times larger than c^* [26]. The degrees of overlapping of precursors before network formation in P-GEL and C-GEL systems are similar because of almost similar values of c. In the case of chemical crosslinking, most of the overlapping of precursor chains leads to trapped entanglements, because the crosslinks are introduced in some monomer units independent of overlapping parts of precursors. By contrast, trapped entanglements in the physical gels will be much fewer than those in the chemical gels, since most of overlapping and spatially adjacent parts of precursors are incorporated into the microcrystallites acting as crosslinks. In fact, the size of the microcrystallites in the transparent physical PVA gels is too small to detect in the moderate range of scattering vector in the neutron scattering experiments [27]. This suggests that each microcrystallite is formed by a small number of monomer units in the overlapped or neighboring part of precursor chains. Owing to little amount of slippery-trapped entanglements along network strands, the finite chain-length effect is expected to appear obviously in the tensile behavior of the physical PVA gels.

4. Concluding remarks

Pure shear deformation reveals the significant differences in the elastic properties of the PVA gels with chemical and physical crosslinks. The ratio of the two principal stresses grows with stretching in the physical gels, while that remains almost constant during deformation in the chemical gels. This difference yields another interesting contrast regarding the elastic free energy (W) between the two gels. The derivative W_2 with respect to the second invariant of the deformation tensor is positive at moderate and large deformation in the chemical gels like most crosslinked rubbers, but that is negative in the whole range of deformation in the physical gels, which is the first observation for elastomers. None of the existing theories of rubber elasticity fully describe the tensile behavior of the physical PVA gels. The negative values of W_2 are qualitatively explained by the non-Gaussian three-chain model considering the finite chain-length effect, although the model fails to describe the difference in the stress–strain behavior among uniaxial, pure shear, and equi-biaxial deformations. These characteristics of the physical PVA gels are expected to originate from the structural features such as fewer trapped entanglements in comparison with the chemical PVA gels.

Acknowledgments

The authors thank Prof. T. Kanaya of Kyoto University for his helpful comments. This work was partly supported by a grant from the 21st century COE program ‘‘COE for a United Approach to New Materials Science’’ from the Ministry of Education, Culture, Sports, Science, and Technology, Japan.

References

[1] de Gennes P-G. Scaling concepts in polymer physics. Ithaca: Cornell University Press; 1979.
[2] Rubinstein M, Colby RH. Polymer physics. New York: Oxford University Press; 2003.
[3] Hyon S-H, Cha W-I, Ikada Y. Polym Bull 1989;22:119.
[4] Takigawa T, Kashihara H, Urayama K, Masuda T. Polymer 1992;33:2334.
[5] Urayama K, Takigawa T, Masuda T. Macromolecules 1993;26:3092.
[6] Kanaya T, Ohkura M, Takeshita H, Kaji H, Furusawa M, Yamaoka H, et al. Macromolecules 1995;28:3168.
[7] Takahashi N, Kanaya T, Nishida K, Kaji K. Polymer 2003;44:4075.
[8] Bastide J, Candau SJ. In: Cohen Addad JP, editor. Physical properties of polymeric gels. John Wiley and Sons; 1996 [chapter 5].
[9] Jones DF, Treloar LRG. J Phys D Appl Phys 1975;8:1285.
[10] Tsuge K, Arenz RJ, Landel RF. Rubber Chem Technol 1978;51:948.
[11] Kawabata S, Matsuda M, Tei K, Kawai H. Macromolecules 1981;14:154.
[12] Fukahori Y, Seki W. Polymer 1992;33:502.
[13] Takigawa T, Yamasaki S, Urayama K, Yamasaki S, Masuda T. Rheol Acta 1996;38:288.
[14] Kawamura T, Urayama K, Kohjiya S. Macromolecules 2001;34:8252.
[15] Kawamura T, Urayama K, Kohjiya S. J Polym Sci Part B Polym Phys 2002;40:2780.
[16] Horkay F, Zrínyi M. Macromolecules 1982;15:1306.
[17] Landau LD, Lifshitz EM. Theory of elasticity. Moscow USSR: Nauka; 1987.
[18] Treloar LRG. The physics of rubber elasticity. 3rd ed. Oxford: Clarendon Press; 1975.
[19] Flory PJ, Rehner J. J Chem Phys 1943;11:512.
[20] Edwards SF. Br Polym J 1977;9:140.
[21] Arruda EM, Boyce MC. J Mech Phys Solids 1993;41:389.
[22] Mao Y. Polymer 1999;40:1167.
[23] Gottlieb M, Gaylord RJ. Macromolecules 1987;20:130.
[24] Urayama K, Kawamura T, Kohjiya S. Macromolecules 2001;34:8261.
[25] Ohkura M, Kanaya T, Kaji K. Polymer 1992;33:3686.
[26] Ferry JD. Viscoelastic properties of polymers. London: John Wiley and Sons; 1980.
[27] Takeshita H, Kanaya T, Nishida K, Kaji K. Physica B 2002;311:78.